

# OAK RIDGE NATIONAL LABORATORY

operated by

UNION CARBIDE CORPORATION

for the

U. S. ATOMIC ENERGY COMMISSION



ORNL-TM- 423

COPY NO. - 53

DATE - Dec. 7, 1962

## A COLLIMATOR STUDY FOR A 5-Gev ELECTRON BEAM

C. D. Zerby and H. S. Moran

### Abstract

A calculation to determine the effectiveness of collimators in a high-energy electron beam is described. Numerical results for a 5-Gev electron beam incident on a 135.42-cm-thick aluminum collimator with an inside radius of 0.85 cm are reported.

### NOTICE

This document contains information of a preliminary nature and was prepared primarily for internal use at the Oak Ridge National Laboratory. It is subject to revision or correction and therefore does not represent a final report. The information is not to be abstracted, reprinted or otherwise given public dissemination without the approval of the ORNL patent branch, Legal and Information Control Department.

LEGAL NOTICE

This report was prepared as an account of Government sponsored work. Neither the United States, nor the Commission, nor any person acting on behalf of the Commission:

- A. Makes any warranty or representation, expressed or implied, with respect to the accuracy, completeness, or usefulness of the information contained in this report, or that the use of any information, apparatus, method, or process disclosed in this report may not infringe privately owned rights; or
- B. Assumes any liabilities with respect to the use of, or for damages resulting from the use of any information, apparatus, method, or process disclosed in this report.

As used in the above, "person acting on behalf of the Commission" includes any employee or contractor of the Commission, or employee of such contractor, to the extent that such employee or contractor of the Commission, or employee of such contractor prepares, disseminates, or provides access to, any information pursuant to his employment or contract with the Commission, or his employment with such contractor.

## Introduction

In high-energy linear electron accelerators the electrons are focused into a narrow beam as they are accelerated down the length of the accelerator tube. The confinement is not absolute, however, and some of the electrons stray out of the beam and are stopped by the tube. This presents a shielding problem over the length of the machine, because the stopped electrons initiate electron-photon cascades, which in turn produce a number of penetrating photo-ejected particles. In addition, the stopped electrons could generate enough heat to require the accelerator tube to be cooled during operation.

At Stanford it has been proposed that constrictions or collimators be placed periodically along the tube of their linear accelerator to strip off the electrons in the outer part of the beam that might otherwise be deposited in the tube. By this procedure it is hoped that the shielding and cooling problems would be restricted to the rather localized regions containing the collimators. With this design there should be some savings in construction costs.

A collimator cannot be constructed to totally absorb the primary and secondary radiations that strike it or are produced in it; hence a certain amount of the radiation is expected to enter the accelerator tube from the body of the collimator and at such an angle as to be sure of hitting the tube downstream. A study is being made at ORNL to determine how radiation behaves in a collimator such as required for the Stanford machine and, in particular, how much radiation is likely to leak back into the accelerator tube from the collimator to be deposited downstream. The three-dimensional electron-photon cascade calculation described previously by Zerby and Moran<sup>1</sup> (to be referred to as ZM-1) was used to consider the collimator problem.

## Geometry

The collimator geometry that could be considered in the calculation is shown in Fig. 1. The parameters  $L_i$ ,  $i = 1, 2, \dots, 20$ , separate

1. C. D. Zerby and H. S. Moran, A Monte Carlo Calculation of the Three-Dimensional Development of High-Energy Electron-Photon Cascade Showers, ORNL-TM-422 (to be published).



the accelerator tube into downstream length intervals for the purpose of recording where radiation strikes the tube. The collimator length is specified as  $T$ , and its inside and outside radius as  $r_1$  and  $r_3$ , respectively. The inside radius of the accelerator tube is specified by  $r_4$ . The radiation that strikes the collimator was assumed to be normally incident at a point a distance  $r_2$  from the center line. All these parameters are specified by the input to the computer program.

#### Calculation of Boundary Effects

Since a photon remains monoenergetic and travels in a straight line as it moves from one point of interaction to another no mathematical difficulty is encountered in the calculation when the photon crosses a boundary. Thus when a photon leaves the collimator and travels down the accelerator tube, it is a simple matter to calculate the position where it hits the tube and its energy at that point. This is not the case for the charged particles.

As pointed out in ZM-1, there is actually a sequence of mathematical operations required in moving a charged particle from one point of interaction to another. First, the distance  $z$  along the initial path of the charged particle is selected, and then the lateral and angular deflection caused by ionization collisions. The particle is moved to the new position determined by  $z$  and the lateral deflection, and then given the new direction determined by the angular deflection. This new position locates the next interaction, and the new direction determines the direction of incidence of the charged particle at the point of interaction.

With the geometry shown in Fig. 1 it is obvious that cases can arise where the initial position of the particle is inside the body of the collimator but the final position is, for example, in the vacuum of the hole. This means that the point where the particle enters the hole and the direction it has at that point must be determined in order to determine where it will travel. (Similar problems arise in the cases of reflection, penetration, lateral escape, and in the case of the path passing through the hole but with its initial and final positions in the body of the collimator.) The techniques used to select the angular and lateral deflections, necessary to the procedure used in the determination, are described below.

As was pointed out in ZM-1, the joint distribution for the lateral and angular deflections is given by

$$f(z, x, \theta_x) dx d\theta_x = \frac{dx d\theta_x}{4\pi B} \exp \left[ \frac{-A_2 \theta_x^2 + 2A_1 x \theta_x - A_0 x^2}{4B} \right], \quad (1)$$

where  $z$  is the distance along the  $z$  axis, which coincides with the original direction of the particle;  $\theta_x$  is the projection on the  $x$  axis of a unit vector along the direction of angular deflection under the assumption that the polar angle of deflection is small;  $x$  is the lateral deflection along the  $x$  axis; and  $A_0$ ,  $A_1$ ,  $A_2$  and  $B$  are functions of  $z$  only. The independent joint-distribution function  $f(z, y, \theta_y)$  is obtained from Eq. 1 by replacing  $x$  and  $\theta_x$  with  $y$  and  $\theta_y$ , respectively.

The distribution function for  $x$  is obtained from Eq. 1 as

$$g(z, x) = \int_{-\infty}^{+\infty} f(z, x, \theta_x) d\theta_x = (4\pi A_2)^{-1/2} \exp \left( \frac{-x^2}{4A_2} \right). \quad (2)$$

The conditional distribution function for  $\theta_x$  is given by

$$h(z, \theta_x | x) = \frac{f(z, x, \theta_x)}{g(z, x)}. \quad (3)$$

The procedure for selecting a random distance  $X$  from the distribution function given in Eq. 2 was to select a random variable  $U_1$  from the distribution  $v(u) = (2\pi)^{-1/2} \exp(-u^2/2)$ , for  $-\infty \leq u \leq +\infty$ , using a standard technique and letting

$$X = [2A_2(z)]^{1/2} U_1. \quad (4)$$

After selecting  $X$  the random variable  $\Theta_x$  can be obtained from the distribution given by Eq. 3 by first selecting  $U_2$  from  $v(u)$  and letting

$$\Theta_x = [2B(z)/A_2(z)]^{1/2} U_2 + A_1(z) [2/A_2(z)]^{1/2} U_1. \quad (5)$$

Equations similar to Eqs. 4 and 5 arise in connection with random selection of  $Y$  and  $\Theta_y$ . For the present discussion, however, it is assumed that  $Y$  and  $\Theta_y$  are both zero and that the problem of crossing a boundary is two-dimensional, as indicated in Fig. 2. It is also assumed that a charged particle starts from point  $O$  and is directed toward  $A$ . The distance  $z$  along this direction is represented by  $OA$ . From Eq. 4 the value of  $X$  is obtained which corresponds to the distance  $AB$  and therefore places the next collision of the particle at  $B$ . As constructed in Fig. 2, the point  $B$  is outside the body of the collimator and the point where the particle left the surface must be calculated. The procedure developed to accomplish this was to proceed along the curve  $OB$  specified by Eq. 4, using an iterative technique until the point  $D$  is reached; the new distance  $z$  corresponding to  $OC$  was then calculated and used in Eq. 5 to select the angle of deflection at the surface.

#### Downstream Acceleration

Once a charged particle enters the accelerator tube downstream from the collimator, the effects of the force field must be considered to accurately determine the point where the charged particle hits the tube and the amount of energy it has at the point of collision. Since the velocities of electrons or positrons approach the velocity of light at relatively low energies ( $\sim 0.5$  Mev), relativistic mechanics must be used to determine the trajectory of the particles.

In the following derivation of the trajectory, the velocity of light,  $c$ , is set equal to unity and the force field is approximated by a constant force,  $F$ , parallel to the  $z$  axis which is along the axis of the tube. The radial displacement of the particle from its initial position is designated as  $\rho$  and the momentum and energy by  $P$  and  $E$ , respectively. The initial energy is taken to be  $E_0$  and the initial projection of  $P$  on the perpendicular to the  $z$  axis to be  $P_\rho$  at the initial position  $z_0$ . Because the force is parallel to the  $z$  axis,  $P_\rho$  remains constant throughout the travel of the charged particle.

UNCLASSIFIED  
ORNL-LR-DWG 72711

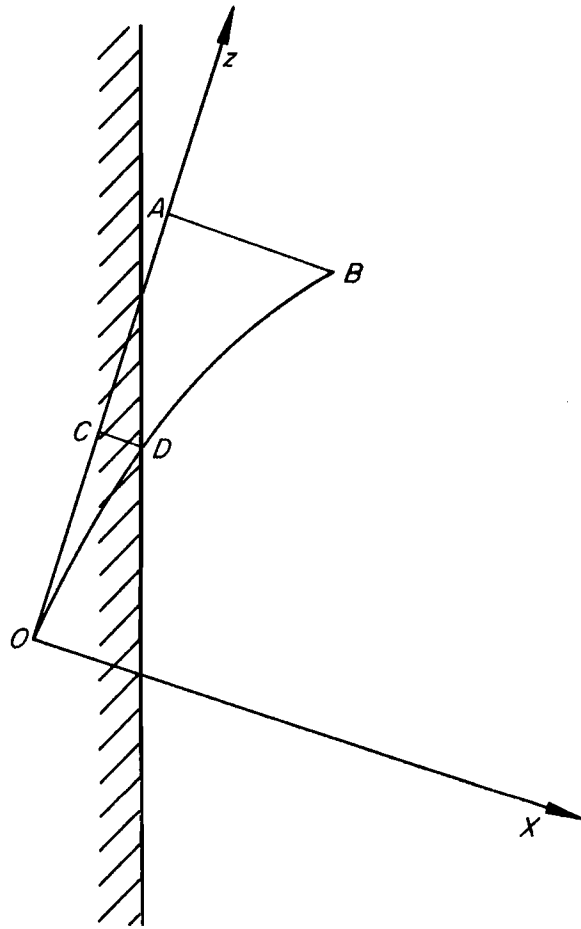


Fig. 2. Schematic Sketch of Boundary Problem.

On the other hand, the projection of  $P$  on the  $z$  axis,  $P_z$ , changes according to

$$F = \frac{dP_z}{dt} . \quad (6)$$

Since  $E = (P_z^2 + P_\rho^2 + m^2)^{1/2}$ , we have that

$$F = \frac{E \frac{dz}{dt} \frac{dE}{dz}}{P_z} = \frac{E v_z \frac{dE}{dz}}{P_z} = \frac{dE}{dz} \quad (7)$$

or that the energy increase per unit length along the axis is a constant.

A useful quantity is the energy of the particle after it travels a certain radial distance,  $\rho$ , from its original position. To obtain the desired relation it should be noted that the radial velocity,  $v_\rho$ , satisfies

$$v_\rho = d\rho/dt = P_\rho/E$$

so that

$$\begin{aligned} d\rho &= \frac{P_\rho}{E} \frac{dz}{dE} \frac{dt}{dz} dE = \frac{P_\rho}{E} \frac{1}{F} \frac{1}{v_z} dE \\ &= \frac{P_\rho}{P_z F} dE = \frac{P_\rho}{F} \frac{dE}{(E^2 - P_\rho^2 - m^2)^{1/2}} . \end{aligned} \quad (8)$$

Integration of Eq. 8 yields

$$\rho = \frac{P_\rho}{F} \ln \left[ \frac{E + (E^2 - P_\rho^2 - m^2)^{1/2}}{E_0 + (E_0^2 - P_\rho^2 - m^2)^{1/2}} \right] , \quad (9)$$

which applies for the case where the particle does not reverse its direction along the  $z$  axis while traveling the distance  $\rho$ ; i.e.,  $E > (P_\rho^2 + m^2)^{1/2}$  for all  $\rho$ . From Eq. 9 we obtain

$$E = \frac{1}{2} \left\{ \left[ E_0 + (E_0^2 - P_\rho^2 - m^2)^{1/2} \right] \exp \left( \frac{\rho F}{P_\rho} \right) + \left[ E_0 - (E_0^2 - P_\rho^2 - m^2)^{1/2} \right] \exp \left( - \frac{\rho F}{P_\rho} \right) \right\} \quad (10)$$

with the restriction

$$\left[ E_0 + (E_0^2 - P_\rho^2 - m^2)^{1/2} \right]^2 \exp \left( \frac{2\rho F}{P_\rho} \right) \geq P_\rho^2 + m^2, \quad (10a)$$

which is only of importance when  $F$  is a negative quantity.

In the calculation, when the charged particle enters the downstream accelerator tube the distance  $\rho$  the particle is required to travel to reach the tube is calculated first. The energy of the particle at the point of collision with the tube is then obtained from Eq. 10 and the distance downstream,  $z$ , where the particle hits is obtained from

$$F = \frac{E - E_0}{z - z_0}. \quad (11)$$

If the particle is a positron, then  $F$  is negative and Eq. 10a is checked to test whether the direction of travel along the  $z$  axis will be reversed in traversing the distance  $\rho$ . If the inequality in Eq. 10a does not hold, then it is assumed that the positron is deposited on the accelerator tube at the distance downstream where its longitudinal motion is reversed because of defocusing forces in the tube. Its energy at this point is  $E = (P_\rho^2 + m^2)^{1/2}$ , and the distance downstream,  $z$ , is obtained from Eq. 11.

### Results

Calculations were performed for an aluminum collimator (density 2.7 g/cm<sup>3</sup> and radiation length 9.03 cm) in the Stanford linear accelerator 2,500 ft from the source. Assuming a constant accelerating

force of  $F = 2 \text{ Mev/ft}$ , the beam energy would be 5 Gev at the collimator. For purposes of accelerating the particles that penetrate the collimator, it was assumed that the accelerating tube and hence the accelerating field extended another 7,500 ft beyond the collimator. In the calculation particles were not accelerated once they passed beyond the end of the tube.

The inside radius of the accelerator tube was taken to be  $r_4 = 1.1303 \text{ cm}$ . The collimator had an outside radius  $r_3 = 50.8 \text{ cm}$ , an inside radius  $r_1 = 0.85 \text{ cm}$ , and a thickness  $T = 135.42 \text{ cm}$  (15 radiation lengths). For purposes of recording where the particles deposited their energy downstream, the tube was divided into nine intervals (see Fig. 1) using  $L_i$  values ( $i = 1, 2, \dots, 9$ ) of 5, 10, 100, 500, 1500, 3000, 4500, 6000, and 7500 ft.

Six cases were run with a 5-GeV beam incident at various points on the collimator as shown in Fig. 1. The values of  $r_2$  selected were 0.85, 0.8528, 0.8556, 0.8780, 0.9901, and 1.1303 cm. A table of the amounts of energy deposited and where they were deposited are given for each case in Table 1. Figures 3 through 7 were constructed using these data.

Figure 3 presents the energy that escapes from the collimator and travels downstream. It is interesting to note that for the larger incident radii, the largest fraction of energy is carried downstream by photons. For  $r_2$  close to  $r_1$ , however, the energy carried by the electrons contributes most because in this case the electrons have a relatively good chance of being scattered into the collimator hole after scattering only a few times in Coulomb collisions.

Figure 4 presents similar data to that presented in Fig. 3 except the effects of the accelerating field on the charged particles have been included. Hence, Fig. 4 presents the energy deposited downstream rather than just the energy escaping from the collimator and traveling downstream. The photon curve is the same in both Figs. 3 and 4, as it should be. Of particular interest in Fig. 4 is the striking difference

Table 1. Energy Distribution for an Aluminum Collimator with an 0.85-cm Inside Radius  
 (Source radiation was 5-Gev electrons normally incident at a point.)

Location	Energy Distribution (Mev/incident particle)				
	Electrons	Positrons	Electrons and Positrons	Photons	Total
$r_2$ , Incident Radius = 0.85 cm					
Absorbed in collimator	-	-	$9.034 \times 10^2$	$5.139 \times 10^1$	$9.548 \times 10^2$
Reflected from face	-	-	0	0	0
Reflected through hole	-	-	0	0	0
Escapes laterally	-	-	$2.568 \times 10^{-2}$	$1.572 \times 10^{-1}$	$1.829 \times 10^{-1}$
Penetrates, but not into accelerator tube	-	-	7.191	$3.011 \times 10^1$	$3.730 \times 10^1$
Penetrates and deposits in downstream interval (ft)					
0-5	$7.762 \times 10^1$	$5.635 \times 10^1$	$1.340 \times 10^2$	$6.358 \times 10^1$	$1.976 \times 10^2$
5-10	$8.044 \times 10^1$	$1.832 \times 10^1$	$9.876 \times 10^1$	$1.708 \times 10^1$	$1.158 \times 10^2$
10-100	$7.025 \times 10^2$	$1.233 \times 10^1$	$7.148 \times 10^2$	$1.010 \times 10^2$	$8.158 \times 10^2$
100-500	$3.208 \times 10^2$	$2.128 \times 10^{-1}$	$3.210 \times 10^2$	$2.218 \times 10^1$	$3.432 \times 10^2$
500-1500	4.425	0	4.425	8.978	$1.340 \times 10^1$
1500-3000	0	0	0	$2.582 \times 10^{-1}$	$2.582 \times 10^{-1}$
3000-4500	0	0	0	0	0
4500-6000	0	0	0	0	0
6000-7500	0	0	0	0	0
7500-∞	$1.028 \times 10^4$	0	$1.028 \times 10^4$	0	$1.028 \times 10^4$

Table 1 (continued)

Location	Energy Distribution (Mev/incident particle)				
	Electrons	Positrons	Electrons and Positrons	Photons	Total
$r_2$ , Incident Radius = 0.852803 cm					
Absorbed in collimator	-	-	$1.944 \times 10^3$	$1.092 \times 10^2$	$2.053 \times 10^3$
Reflected from face	-	-	0	$4.793 \times 10^{-3}$	$4.793 \times 10^{-3}$
Reflected through hole	-	-	0	0	0
Escapes laterally	-	-	0	$4.285 \times 10^{-1}$	$4.285 \times 10^{-1}$
Penetrates, but not into accelerator tube	-	-	$1.743 \times 10^1$	$6.723 \times 10^1$	$8.466 \times 10^1$
Penetrates and deposits in downstream interval (ft)					
0-5	$2.085 \times 10^2$	$9.124 \times 10^1$	$2.997 \times 10^2$	$1.192 \times 10^2$	$4.189 \times 10^2$
5-10	$3.415 \times 10^2$	$4.291 \times 10^1$	$3.844 \times 10^2$	$1.031 \times 10^2$	$4.875 \times 10^2$
10-100	$1.317 \times 10^3$	$4.853 \times 10^1$	$1.366 \times 10^3$	$5.609 \times 10^2$	$1.927 \times 10^3$
100-500	6.103	1.345	7.448	$5.409 \times 10^1$	$6.154 \times 10^1$
500-1500	0	0	0	$1.427 \times 10^{-1}$	$1.427 \times 10^{-1}$
1500-3000	0	0	0	0	0
3000-4500	0	0	0	0	0
4500-6000	0	0	0	0	0
6000-7500	0	0	0	0	0
7500-∞	$2.502 \times 10^1$	0	$2.502 \times 10^1$	0	$2.502 \times 10^1$
$r_2$ , Incident Radius = 0.855606 cm					
Absorbed in collimator	-	-	$2.371 \times 10^3$	$1.342 \times 10^2$	$2.505 \times 10^3$
Reflected from face	-	-	0	0	0

Table 1 (continued)

Location	Energy Distribution (Mev/incident particle)				
	Electrons	Positrons	Electrons and Positrons	Photons	Total
Reflected through hole	-	-	0	0	0
Escapes laterally	-	-	0	$4.247 \times 10^{-1}$	$4.247 \times 10^{-1}$
Penetrates, but not into accelerator tube	-	-	$1.831 \times 10^1$	$8.213 \times 10^1$	$1.004 \times 10^2$
Penetrates and deposits in downstream interval (ft)					
0-5	$2.522 \times 10^2$	$9.397 \times 10^1$	$3.462 \times 10^2$	$1.390 \times 10^2$	$4.852 \times 10^2$
5-10	$4.037 \times 10^2$	$3.113 \times 10^1$	$4.348 \times 10^2$	$1.201 \times 10^2$	$5.549 \times 10^2$
10-100	$7.171 \times 10^2$	$5.846 \times 10^1$	$7.756 \times 10^2$	$5.873 \times 10^2$	$1.363 \times 10^3$
100-500	0	0	0	$1.496 \times 10^1$	$1.496 \times 10^1$
500-1500	3.699	0	3.699	0	3.699
1500-3000	0	0	0	0	0
3000-4500	0	0	0	0	0
4500-6000	0	0	0	0	0
6000-7500	0	0	0	0	0
7500-∞	0	0	0	0	0
$r_2$ , Incident Radius = 0.87803 cm					
Absorbed in collimator	-	-	$3.253 \times 10^3$	$1.833 \times 10^2$	$3.436 \times 10^3$
Reflected from face	-	-	0	$2.717 \times 10^{-2}$	$2.717 \times 10^{-2}$
Reflected through hole	-	-	0	0	0
Escapes laterally	-	-	0	$5.372 \times 10^{-1}$	$5.372 \times 10^{-1}$
Penetrates, but not into accelerator tube	-	-	$2.068 \times 10^1$	$1.057 \times 10^2$	$1.264 \times 10^2$

Table 1 (continued)

Location	Energy Distribution (Mev/incident particle)				
	Electrons	Positrons	Electrons and Positrons	Photons	Total
Penetrates and deposits in downstream interval (ft)					
0-5	$3.792 \times 10^2$	$1.304 \times 10^2$	$5.096 \times 10^2$	$2.581 \times 10^2$	$7.677 \times 10^2$
5-10	$1.392 \times 10^2$	$3.590 \times 10^1$	$1.751 \times 10^2$	$1.803 \times 10^2$	$3.554 \times 10^2$
10-100	$6.326 \times 10^1$	$1.143 \times 10^1$	$7.469 \times 10^1$	$2.562 \times 10^2$	$3.308 \times 10^2$
100-500	0	0	0	$5.631 \times 10^{-2}$	$5.631 \times 10^{-2}$
500-1500	0	0	0	0	0
1500-3000	0	0	0	0	0
3000-4500	0	0	0	0	0
4500-6000	0	0	0	0	0
6000-7500	0	0	0	0	0
7500-∞	0	0	0	0	0
$r_2$ , Incident Radius = 0.99015 cm					
Absorbed in collimator	-	-	$4.244 \times 10^3$	$2.418 \times 10^2$	$4.486 \times 10^3$
Reflected from face	-	-	0	0	0
Reflected through hole	-	-	0	0	0
Escapes laterally	-	-	0	1.213	1.213
Penetrates, but not into accelerator tube	-	-	$2.376 \times 10^1$	$1.116 \times 10^2$	$1.354 \times 10^2$
Penetrates and deposits in downstream interval (ft)					
0-5	$5.049 \times 10^1$	$2.732 \times 10^1$	$7.781 \times 10^1$	$2.088 \times 10^2$	$2.866 \times 10^2$
5-10	$4.046 \times 10^{-1}$	$1.027 \times 10^1$	$1.067 \times 10^1$	$5.563 \times 10^1$	$6.630 \times 10^1$

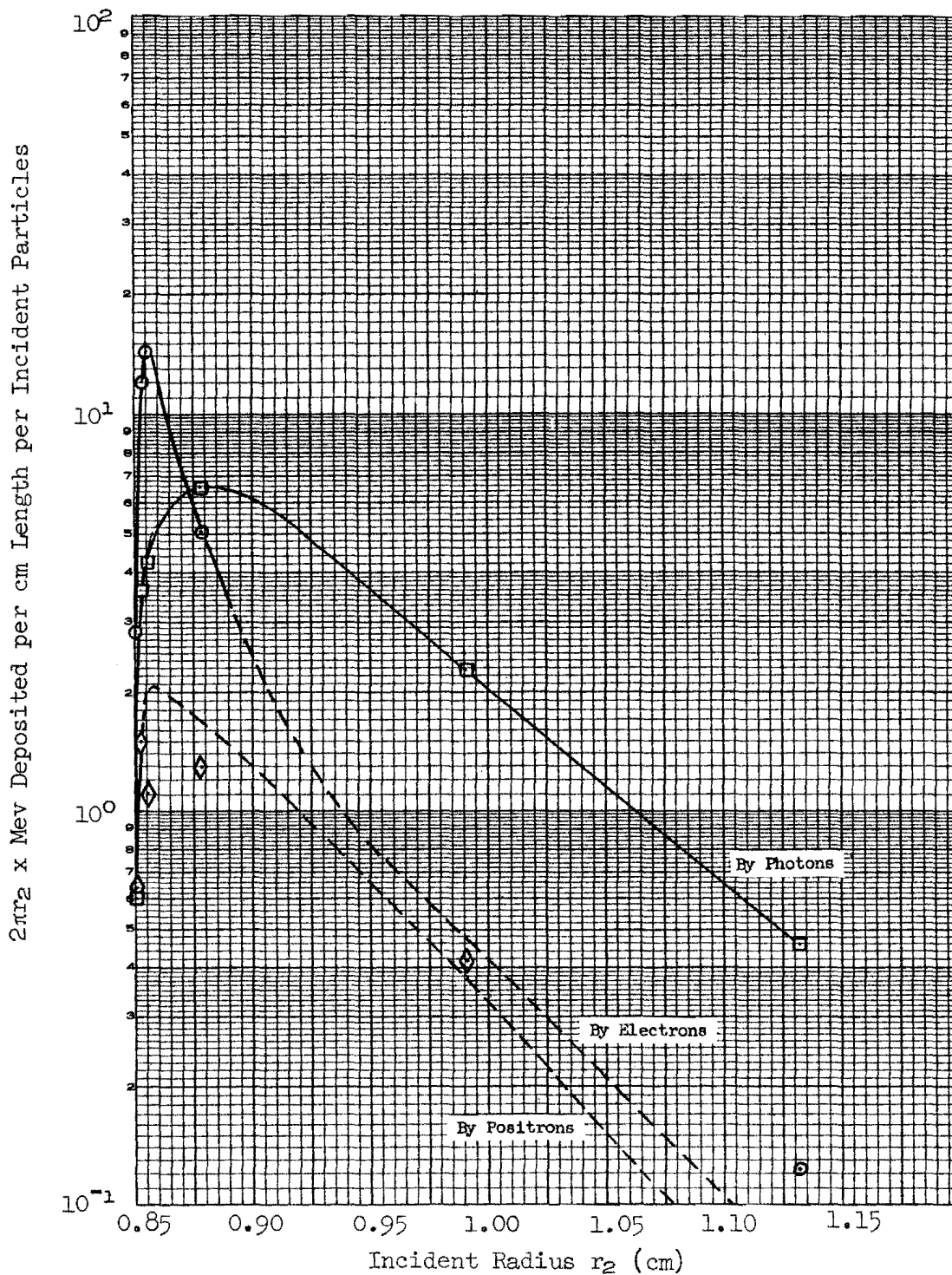


Fig. 6. Energy Deposited Per cm Length in the 5 to 10 ft Interval of the Accelerator Tube by Radiation Escaping from a 135.42-cm-Thick Aluminum Collimator with 0.85-cm Inside Radius. The effects of the downstream accelerating field are included. Source radiation was 5-GeV electrons.

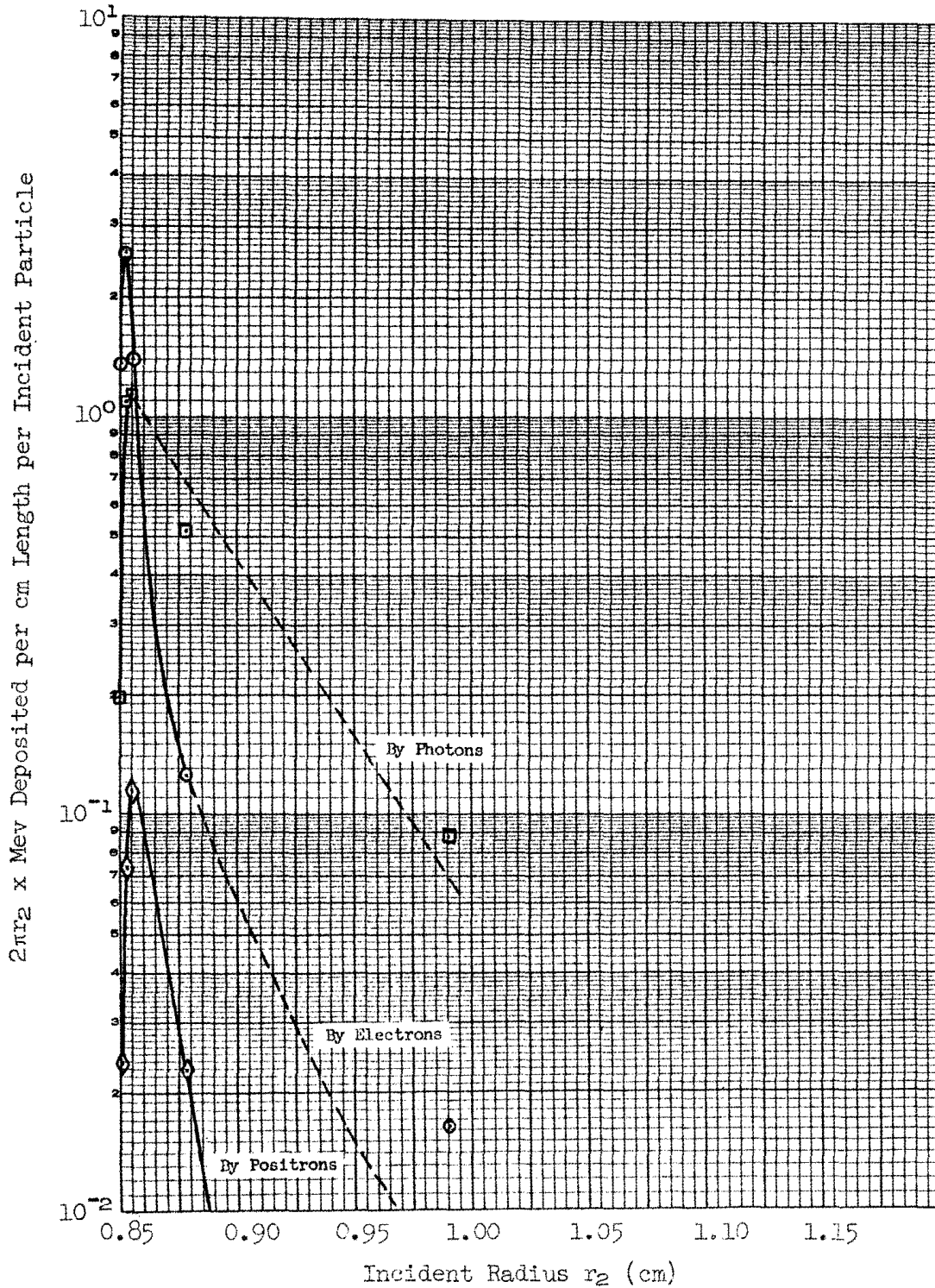


Fig. 7. Energy Deposited Per cm Length in the 10 to 100 ft interval of the Accelerator Tube by Radiation Escaping from a 135.42-MeV Aluminum Collimator with a 0.85-cm Inside Radius. The effects of the downstream accelerating field are included. Source was 5-GeV electrons.

Table 2. Energy Deposited in Accelerator Tube by Radiation Leaving the Body of the Collimator (Source radiation was uniformly distributed 5-Gev electron beam normalized to one source particle; collimator described in the text.)

Particles	Energy Deposited (Mev)		
	Location		
	0 to 5 ft	5 to 10 ft	Total Tube
Photons	81.8	30.3	146.2
Electrons	43.9	19.0	96.6
Positrons	19.0	6.9	25.9
Total	144.7	56.2	268.7

Internal Distribution

- |                         |  |
|-------------------------|--|
| 1. F. S. Alsmiller      | 14. R. W. Peelle   |
| 2. R. G. Alsmiller, Jr. | 15. S. K. Penny  |
| 3. H. W. Bertini        | 16. D. K. Trubey   |
| 4. E. P. Blizard        | 17-26. C. D. Zerby   |
| 5. F. Clark             | 27. W. Zobel   |
| 6. R. R. Coveyou        | 28-52. Laboratory Records                                    |
| 7. L. Dresner           | 53. Laboratory Records, ORNL R.C.                            |
| 8. W. A. Gibson         | 54-55. Central Research Library                              |
| 9. W. H. Jordan         | 56. Document Reference Section                               |
| 10. F. B. K. Kam        | 57-72. Division of Technical<br>Information Extension (DTIE) |
| 11. W. E. Kinney        | 73. Research and Development<br>(ORO)                        |
| 12. F. C. Maienschein   |  |
| 13. H. S. Moran         |  |

External Distribution

74. Herman J. Schaefer; U.S. Naval School of Aviation, Pensacola, Fla.
75. S. P. Shen; New York University, University Heights, New York, N.Y.
76. E. A. Cosbie; Argonne National Laboratory, Argonne, Illinois
- 77-79. B. J. Moyer, R. Wallace, and W. Patterson; University of California Radiation Laboratory, Berkeley, California
- 80-81. K. G. Dedrick and W. K. H. Panofsky; Stanford Linear Accelerator Center, Stanford University, Stanford, California
- 82-86. H. DeStaebler, Jr.; Stanford Linear Accelerator Center, Stanford University, Stanford, California
- 87-91. R. F. Mozley; Stanford Linear Accelerator Center, Stanford University, Stanford, California
92. M. S. Livingston, Cambridge Electron Accelerator, 42 Oxford Street, Cambridge 38, Massachusetts
93. W. N. Hess; NASA, Goddard Space Flight Center, Greenbelt, Maryland
94. O. L. Tiffany; Bendix Systems Division, The Bendix Corporation, Ann Arbor, Michigan
95. R. L. Childers; University of Tennessee, Knoxville, Tennessee
96. A. Galonsky; Midwestern Universities, Research Association, 2203 University Avenue, Madison 5, Wisconsin
- 97-98. F. P. Cowan and S. J. Lindenbaum; Brookhaven National Laboratory, Upton, Long Island, New York
99. H. B. Knowles; Yale University, Sloane Laboratory, New Haven, Connecticut
100. R. B. Curtis; Indiana University, Bloomington, Indiana
101. J. S. Russ; Palmer Physical Laboratory, Princeton University, Princeton, New Jersey

